

Paragenetic conditions of concretions in the Neogene clastic sediments of NW Borneo: Evidence from morphological, petrographic, mineralogical and geochemical data

R. Nagarajan^{1,2*}, R. Sharveen¹, Abdulmajid Ali¹, F.L. Kessler³, John Jong⁴, P.D. Roy⁵ and S. Srinivasalu⁶

¹Department of Applied Sciences (Applied Geology), Curtin University, CDT 250, Miri Sarawak, Malaysia

²Curtin Malaysia Research Institute, Curtin University, Malaysia

³Goldbach Geoconsultants O & G, Glattbach, Aschaffenburg, Germany

⁴JX Nippon Oil and Gas Exploration (Malaysia) Limited, Kuala Lumpur, Malaysia

⁵Instituto de Geología, Universidad Nacional Autónoma de México (UNAM), Ciudad Universitaria
C.P. 04510, Coyoacan, México DF., México

⁶Department of Geology, Anna University, Chennai – 25, India

*Corresponding author: nagarajan@curtin.edu.my; nagageochem@yahoo.com

Abstract: Concretions are hard and compact inorganic masses, formed within the sedimentary sequences by the precipitation of mineral cement within the spaces between the sediment grains through diagenesis and pore fluids. Concretions often yield valuable records for the post-depositional changes in sedimentary units since they preserve valuable evidence of groundwater flow and water-rock interactions which resulted in mineral dissolution and precipitation. 30 pyrite concretion samples were selected from the 36 total concretion samples collected from the Tukai Formation, NW Borneo, Malaysia and were studied to understand their morphology and paleoenvironment. Interbedded sandstone and mudstone sequences from the Tukai Formation contain a variety of early diagenetic pyrite concretion morphologies, including elongate and tabular concretions of variable shapes. The present preliminary study reports the geochemistry and mineralogy of pyrite concretions from the Neogene sedimentary sequences of NW Borneo. In the present study, five different types of concretion were collected from mostly clay and coal interbedded sandstone beds, which are circular (1.5-4cm), elongate (0.5-1cm diameter; 4-6cm length), tabular (4-5cm diameter), spherical (1.5-2.5cm) heterolithic (2-2.5cm diameter; 8cm length) and irregular (14 × 11cm) shapes. The nucleus and layers were observed inside the spherical and irregularly shaped concretions respectively, and the nucleus mainly consists of organic matter. X-ray diffraction (XRD) analysis showed that the concretions are composed mainly of quartz, and pyrite, and some samples show other minerals i.e. catterite, goethite, berlinite, and arsenopyrite. Chemically these concretions are enriched with Fe₂O₃, total Sulphur, SiO₂, and trace elements such as Mo, Nb, As, Pb, Zr, Sr, and Rb. Mn and Ni are recorded high, however, only three samples have recorded these elements. The high content of Fe₂O₃, total Sulphur and SiO₂ in these concretions are clearly related to mineralogy (i.e. mainly of pyrite and quartz). Pyrite-dominated concretions can be related to near-surface and burial diagenesis of organic matter from the coal beds. The existence of pyrite occurred as clusters of individual crystals within concretion suggesting that they were formed significantly under reducing conditions (microbial sulphate reduction) during early diagenesis or replacement of Fe(hydr)oxides and the sulfidation mechanism with the aid of FeS precursor during the diagenetic process. However, a more detailed study is required to confirm the diagenetic paleoenvironments and controlling factors of the development of these pyrite concretions from the Tukai Formation.

Keywords: Concretions, Neogene sediments, Tukai Formation, Borneo.

Introduction

Concretions are the hard and compact inorganic masses which are precipitated mineral cements within the spaces between the sediment grains through diagenesis and pore fluids within the sedimentary rocks. Concretions form in different shapes, sizes, hardness, and colours and are reported worldwide (Chan et al., 2004, 2007; England et al., 2002; Ehinola et al., 2010; Potter et al., 2011; Wilson et al., 2012; He et al., 2019; Xu et al., 2020). They are usually spherical and/or disk-shaped, embedded in a host rocks with different compositions and also occur in other shapes (tabular, discs-like, spheroidal and cylindrical). Nucleation and growth of concretions is possible in variable depths in the subsurface (up to 3-4km depth; Milliken et al., 1998) and also near the sediment-water interface (Raiswell and Fisher, 2000). The natural spherical balls are called nodules and/or concretions with the name of the minerals, which are enriched in the particular balls (Iron concretion, Pyrite concretions, Mn nodules, etc.).

Pyrite concretions are often reported in marine sediments and lacustrine environments, and they are formed through the involvement of microbial sulphate reduction, changes in pH and redox conditions (Driscoll et al., 1965; Raiswell, 1976; Pye et al., 1990). Often, Concretions form in a localised microenvironments, and sometimes can be developed by organism decay (Woodland and Stenstrom, 1979; Baird et al., 1986). Concretions often yield valuable records about the post-depositional changes in sedimentary units since they have preserved valuable information of groundwater flow and water-rock interactions, which resulted in mineral dissolution and precipitation (El Albani et al., 2001; Chan et al., 2007). There are many studies have separated concretion into three main types which are syngenetic, diagenetic and epigenetic (He et al., 2019). The concretion formation mechanism remains enigmatic. Based on the tripartite geochemical fluid flow model, Chan et al. (2000, 2005), have described the source of Fe, iron mobilisation and the precipitation cycle of iron being reflected on the concretion geometrics and its diagenetic facies. First is, the source of iron: Fe³⁺ was

precipitated as early diagenetic grain coatings retrieved from the removal of detrital ferromagnesian minerals. The second is on iron mobilization, a reducing fluid penetrated the sandstone, and the iron was mobilized into a solution as Fe^{2+} . The third is the iron precipitation, the iron-bearing and the reducing fluids integrated with an oxidizing fluid that precipitates Fe^{3+} into hydrous ferric oxide (HFO) elements.

Though many studies have been carried out on concretions from other parts of the world (Pantin, 1958; Berner and Raiswell 1983; Raiswell, 1976; Coleman and Raiswell, 1981, 1995; Mozley, 1989; Huggett, 1994; Chan et al., 2000, 2004, 2005, 2007; Bowen et al., 2008; Potter et al., 2011; He et al., 2019; Xu et al., 2020), no or less study has been undertaken from NW Borneo. The previous studies mainly addressed the geochemical constraints in terms of provenance, recycling and weathering (Nagarajan et al., 2014; 2017a); mineralogical variations (Nagarajan et al., 2017b) and semi-quantitative assessment of clay content in the clastic rocks of the Tukai Formation (Kessler and Nagarajan, 2012, 2013). Clay, mudstone and coal-interbedded sandstones of the Tukai formation contain a variety of early diagenetic iron sulphide morphologies, which belongs to the Neogene age (Hutchison, 2005). Thus, our preliminary study reports the geometry, mineralogy, and geochemistry of pyrite concretions from NW Borneo to understand their morphology and paleoenvironment.

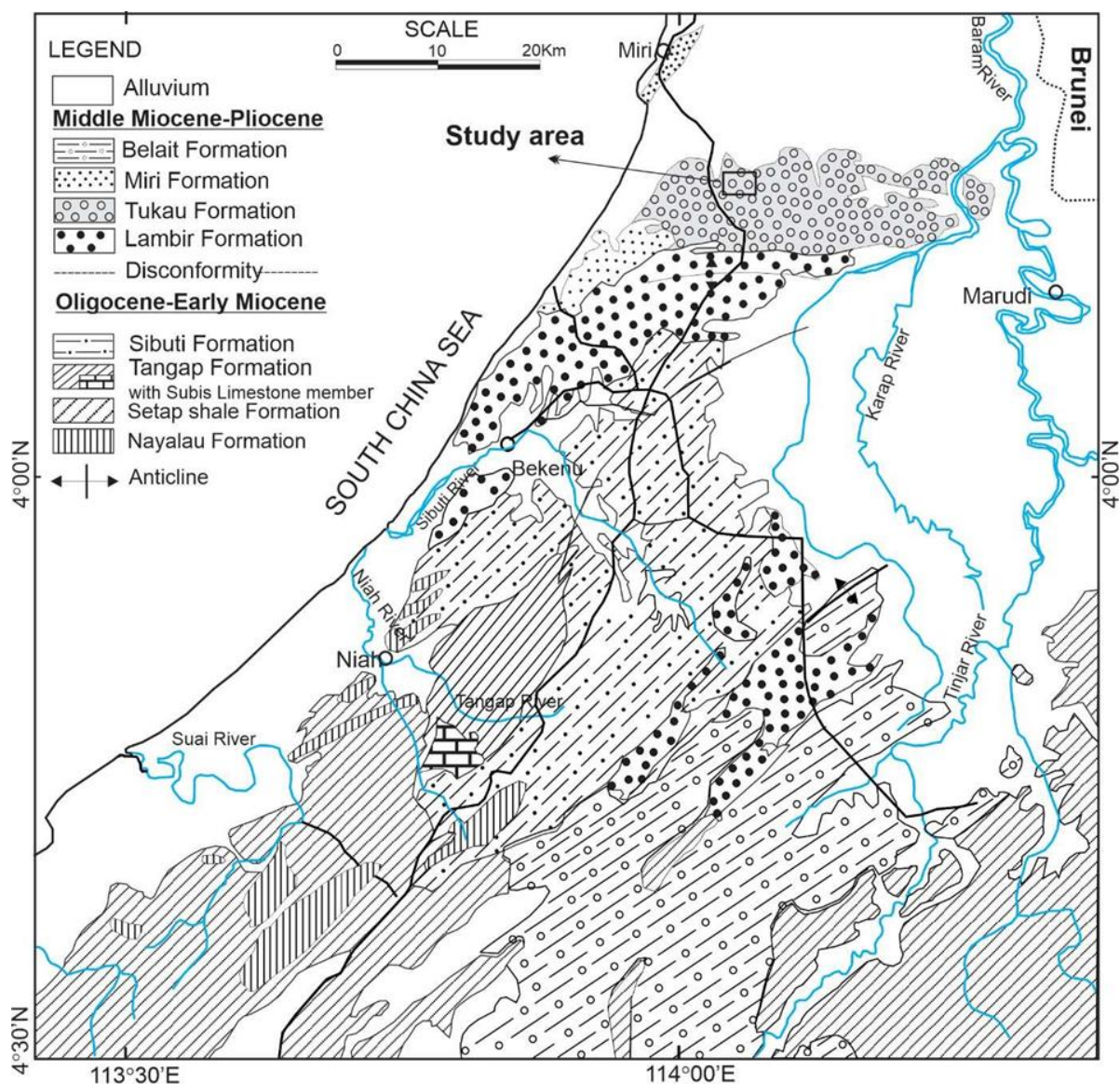


Fig. 1. Geology map of northern Sarawak showing the location of the study area (after Liechti et al., 1960; modified from Nagarajan et al., 2015).

Study Area

The Tukau Formation and its sedimentary sequences are preserved in a relatively simple synclinal structure with a number of young compressive and strike-slip fault systems dissecting it. It has a thickness of several hundreds of meters and consists of clay/mudstone and sandstone beds with coal laminations. The lenticular-shaped channelized deposits are observed in both at the lowermost and the upper parts of the formation, which are composed of medium to coarse-grained sandstones with rare micro-conglomerates at the channel base, representing a shore face environment of deposition (Kessler, 2010). In general foraminifers (except for some brackish water forms) are absent and the lignite layers and amber balls present in layered strata, which suggest a coastal plain environment (Hutchison, 2005). Similarly, Wilford (1961) reported the brackish water fauna such as *Ammobaculites sp.*, *Trachamiina sp.*, *Haplophragmoides sp.* and *Glomospira sp.* and found that which cannot be used for the chronology of the host sediments. However, the Tukau Formation’s age ranges between Upper Miocene and Lower Pliocene and it conformably overlies the Lambir Formation next to Sungai Liku in the eastern Lambir Hill, which belongs to the Middle to Late Miocene.

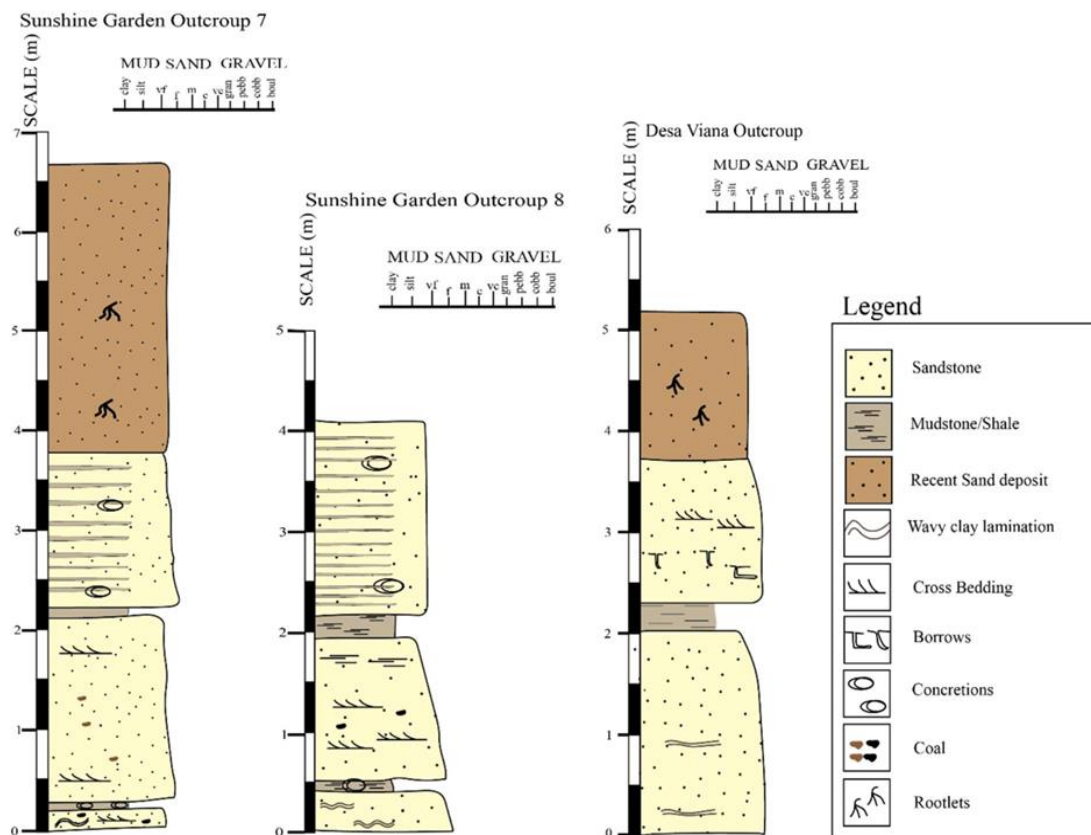


Fig. 2. The stratigraphic logs of the studied sections, Tukau Formation.

Materials and Methods

In total, 36 concretion samples were collected from three well-exposed outcrops (Sunshine Garden: three outcrops; coordinates: 477537.38N, 829564.42E; 477478.46N, 829592.43E; 476640.46N, 828995.69E) of the Tukau Formation (on the route from Luak to Tukau) (Figs. 1 and 2). Concretions were mostly associated with shale/mudstone and clay layers interbedded sandstones and also collected from the surface (separated by weathering and erosion) (Fig. 2). Out of 36 concretion samples, thirty fresh samples were selected for bulk geochemical and XRD analyses. Samples were chosen based on size and shape and intensity of oxidation. Selected samples underwent a cleaning process, where only samples of fresh or unweathered rocks are used for analysis. Weathered portions were then removed for all the concretions except oxidized and heterolithic concretions with the use of a pen knife with gloves on. All samples were then dried at a room temperature of <30°C. After which, they were placed in sample bags and pounded, crushed and grinded using agate mortar to a size of 75 microns. XRD

analysis was performed using the PANalytical Empyrean X-Ray Diffractometer. Samples were analysed in the 2 Theta range of 5° and 70° using Cu-tube as the X-ray source and standard generator setting of 40mA and 45kV. After this, the peaks were then identified using “highscore”.

The major oxides were analysed using fused discs while trace elements were analyzed in pressed pellets as per the methods of Verma et al. (1996) and Lozano and Bernal (2005) using Siemens SRS 3000 wavelength dispersive X-ray fluorescence (XRF) spectrometer. Triplicate analysis was performed and the relative error for the duplicate samples was between 1 and 5%. The precision of the analysis was <10% for both major and trace elements (Roy et al., 2010; Kessler and Nagarajan, 2012; Nagarajan et al., 2017). The sedimentary rocks of the Tukai Formation (n=5) and one sample each for various concretion types (n=9) were studied for their petrography by preparing thin sections and the thin sections were studied using Nikon Eclipse LV100NPOL polarizing microscope.

Statistical analyses such as Pearson correlation and Varimax rotated principal component analysis were carried out using SPSS 17 software (e.g. Jayaprakash et al., 2014; Ramkumar, 2001). The correlation coefficient “r” values >0.5 and the significant level of p<0.05 were considered for the present analysis. The factors with an Eigenvalue greater than 1 (Kaiser, 1960) were considered for interpretation.

Results

Field data

The lithology of each outcrop was identified as grey sand (lower part) shale unit, inter-bedded sandstone/shale, clean sand and top covered by residual soil and vegetation. Sandstone layers show cross-bedding, and thin coal laminae were observed parallel to cross-bedding. Ripple marks can be found at the lower part of the grey sand unit. Concretions were mostly found to be associated with shale/mudstone beds and interbedded sandstone units (Fig. 2). Also, amber balls are also commonly observed in the Tukai Formation. Trace fossils consisting of burrows can mostly be seen in clean sand layers and are absent in shale/mudstone layers. Paleo current directions were measured in all the studied outcrops (at least 20 measurements) and plotted in a rose diagram, which shows the direction towards NNW with minimum distribution towards NNE. The physical appearance and descriptions of the concretions are summarized in Table 1.

Mineralogy

Twenty-six out of twenty 28 samples show their mineral composition rich in quartz associated with pyrite except for two heterolithic samples where quartz was associated with other pyrite minerals such as catterite or goethite (altered from pyrite) at the edge (Table 1). The minerals precipitated in the concretion can be best explained by the cementation of minerals in the pore space. The different intensities of red coloration can be seen, reflecting the fact that most hematite/marcasite forms after concretion was formed. Fe is often leached from pyrite minerals in the concretions and then redeposits as cement in heterolithic and weathered concretions.

Petrography

The matrix of the elongated concretions is dominated by quartz in the silt fraction. A minor amount of clay and pyrite are found in most of the samples. Shell fragments are extremely rare. Petrographically the concretion consists of quartz, pyrite, Fe-cement and some lithic fragments with good porosity. Quartz varies between anhedral and subhedral in nature and shows polycrystalline grains with undulose extinctions. Fractures are common in quartz grains. Pyrites are opaque in nature and are leached to Fe-cement, which coated the quartz grains and is also common along the edges of pyrite grains. Some lithic fragments are also seen, which are siltstone and mudstone. Porosity was estimated to be 20%, of which, 70 % is interconnected, remaining is isolated porosity. Mineral grains range from 0.05 mm to 0.5mm in diameter.

Geochemistry

The bulk geochemistry of the concretions based on the morphological classification is summarised in Table 2. The pyrite concretion of the present study shows a high concentration of Fe₂O₃, SiO₂, total S,

Mo, Nb, Mn, As, Pb, and Zr. Fe₂O₃ was recorded higher in circular, tabular, spherical (minimum variation) and heterolithic concretions (wide variation). Fe₂O₃ content is mostly similar in all concretions (Max avg: 28.6% in spherical and min avg. 6.1% in coarse-grained irregular concretions) except heterolithic fresh concretions (Table 2). Total sulphur is the second dominant element recorded higher in spherical (15.3%) tabular (14.9%) and circular (14.6%) concretions compared to other concretions. SiO₂ ranges between 14.6% (Coarse-grained irregular concretions) and 6.7% (Heterolithic core). The abundance of iron, total sulphur and silica in concretions can be summarized as follows:

$$\begin{aligned} \text{Fe}_2\text{O}_3 &= \text{SP} > \text{Cir} > \text{Tab} > \text{HEdge} > \text{Elong} > \text{Oxi} > \text{HCore} > \text{CG} > \text{HF} \\ \text{Total Sulphur} &= \text{Sp} > \text{Tab} > \text{Cir} > \text{CG} > \text{HCore} > \text{HF} > \text{Hedge} > \text{Elong} > \text{Oxi} \\ \text{SiO}_2 &= \text{CG} > \text{HF} > \text{Tab} > \text{Cir} > \text{SP} > \text{Elog} > \text{Hedge} > \text{Oxi} > \text{Hcore} \end{aligned}$$

Trace elements such as Mn, Mo, As, Ni, Pb and Nb are recorded higher in the concretions than Rb and Sr. Even though Mn and Ni are recorded higher than other trace elements, the higher concentrations are recorded only in circular, spherical and tabular concretions. Mo is recorded in the range between 125 ppm (Heterolithic fresh) and 348 ppm (circular concretions). As also recorded higher and ranges between BDL and 395ppm (heterolithic core). Pb content is comparable among the concretions and is in the range of 40 - 70 ppm in heterolithic fresh and heterolith core concretions respectively.

Table 1. Summary of concretion’s physical appearance and mineralogy (by XRD).

Sample type	Hardness	Physical appearance	Mineralogy
Elongated	High	No distinct pyrites.	Quartz, Pyrite
Tabular	Moderate	Pyrite or marcasite crystals are concentrated on a certain part of the surface. Usually found along the clay bedding from the formation.	Quartz, Pyrite, Arsenopyrite
Spherical	Very high	Fully or mostly pyrite and/or marcasite minerals were observed and sometimes dispersed around the sphere. Cause sparkling when hammered. The outer part is frequently surrounded by higher Fe-coated sand material.	Quartz, Pyrite
Circular	Moderate	Distinct either pyrite or marcasite on the surface. The outer part is frequently surrounded by higher Fe-coated sand material.	Quartz, Pyrite
Heterolithic	Moderate	Different material between core and edge. Core part presumable consists of organic material while the outer part is frequently surrounded by high Fe sand material.	Quartz, pyrite, Cattierite, Goethite
Coarse grained concretions	Low	Very coarse-grained, compacted up to pebble size quartz, composed mainly of quartz and often very loose and easily broken.	Quartz, Pyrite
Oxidized forms	Low	A brittle and weathered surface forms white fibrous matter. Strong sulphur odor.	Quartz, Pyrite, Berlinite

Discussion

Concretion Morphology

Concretion’s geometry is the result of a complex interaction between diffusive and advective mass transfer (Potter et al., 2011). The distinctive concretions formed in clastic sediments stand out since their mineral composition is different from that of the bulk rock (Coleman, 2005). Pyrite concretions in the Tukai Formation consist of bright, lustrous, tiny interlocked crystals in more complex and interesting shapes. Pyrite concretions were observed on cut surfaces and their sizes were measured and classified based on their shape. The surfaces of the concretions show different colours, i.e. grey, yellow,

brown, yellowish brown and metallic whereas the inner part of the concretions mostly displays grey and black colour (Fig. 3). The brownish-yellow is due to weathering of pyrite minerals from the concretions. Most of the concretions are generally spherical, the pyrite most often exhibits dull-colour, massive or granular forms. In the present study, five different types of concretion are collected from mostly shale and interbedded shale/sandstone beds, which are circular (1.5-4cm), elongate (0.5-1cm diameter; 4-6cm length), tabular (4-5cm diameter), spherical (1.5-2.5cm) and heterolithic (2-2.5cm diameter; 8cm length) shapes (Fig. 3). The elongated concretions show a similar alignment of bedrock.

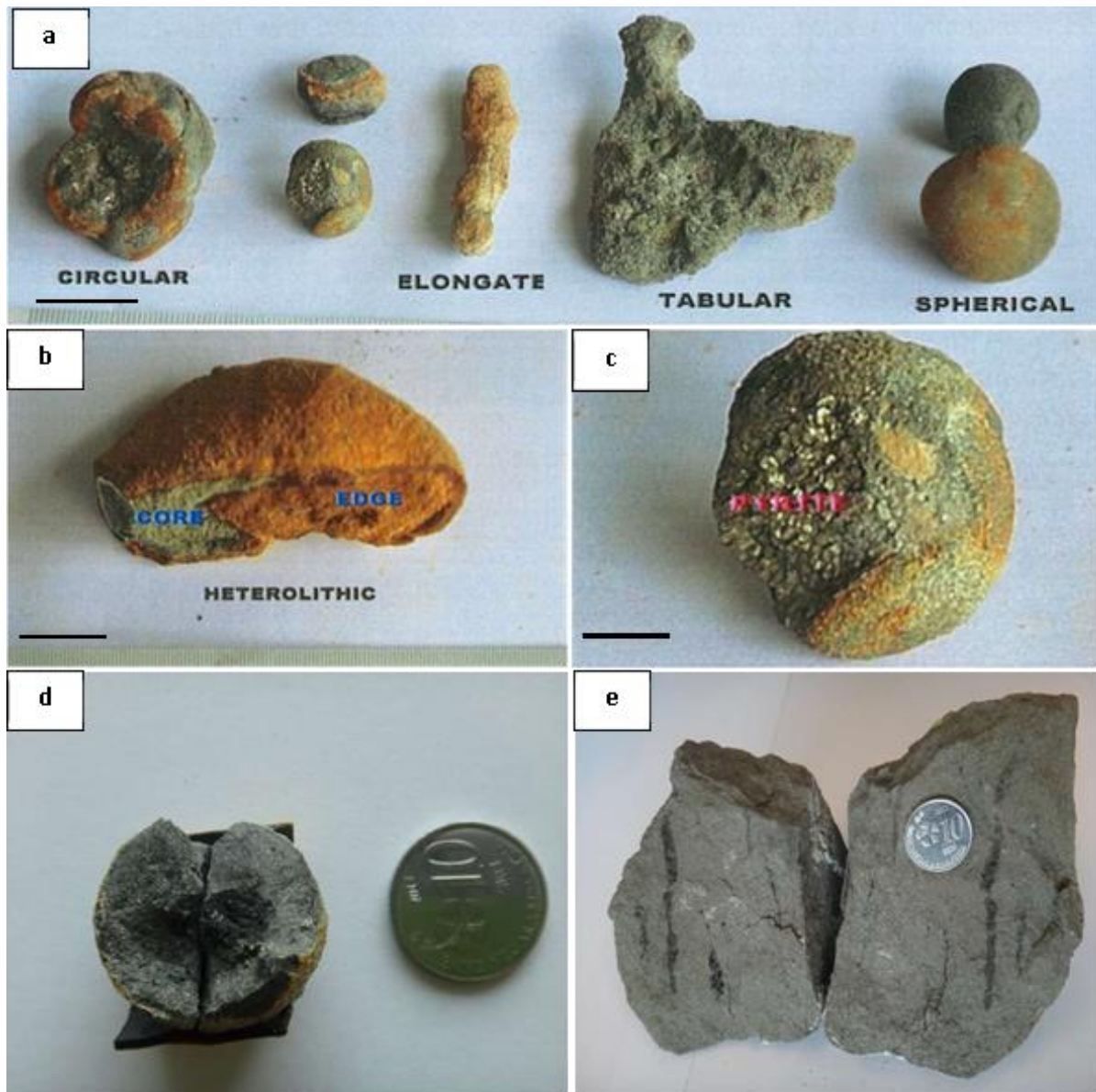


Fig. 3a-e. Photographs of different varieties of concretions from Tukai Formation, NW Borneo (Scale: scale bar = 2cm; Coin diameter=1.8cm)

According to Chan et al. (2007) internal structure of concretions can be divided into three types: solid, rind and layered. Concretions from the Tukai Formation mostly show a solid internal structure, made up of quartz and pyrite. Solidly structured concretions do not show any particular internal pattern and are cemented evenly (Chan et al., 2007; Potter et al., 2011). Homogenized host rock creates an even distribution of diffusion mass transfer of ions, which allows the concretion to grow evenly as a spherical shape (Seilacher, 2001; Mozley and Davis, 2005; Potter et al., 2011).

Table 2. Bulk geochemistry of various morphology of pyrite concretions from the Tukau Formation.

Oxides/ elements	Circular (n=4)				Spherical 1 (n=4)				Tabular (n=5)				Heterolithic edge (n=3)				
	Min	Max	Avg	St. Dev	Min	Max	Avg	St. Dev	Min	Max	Avg	St. Dev	Min	Max	Avg	St. Dev	
Fe ₂ O ₃	24.7	32.3	28.4	3.8	27.2	30.0	28.6	1.5	25.7	31.0	27.7	2.0	20.3	28.7	25.9	4.9	
CaO	0.08	0.14	0.10	0.03	0.08	0.11	0.10	0.01	0.07	0.10	0.09	0.01	0.07	0.11	0.09	0.02	
K ₂ O	0.02	0.03	0.02	0.01	0.02	0.022	0.02	0.00	0.02	0.02	0.02	0.00	0.01	0.02	0.02	0.01	
SiO ₂	8.3	12.0	10.2	1.9	8.2	11.5	9.2	1.5	7.4	14.2	10.5	2.6	6.0	9.6	8.1	1.8	
∑ S	12.5	17.6	14.6	2.3	14.0	17.1	15.3	1.5	13.1	16.6	14.9	1.5	0.4	14.9	9.9	8.2	
Cl	0.1	0.2	0.1	0.0	0.1	0.2	0.1	0.0	0.1	0.1	0.1	0.0	0.1	0.2	0.1	0.0	
Mo	200	450	348	110	240	410	338	86	230	330	280	45	130	380	287	137	
Nb	150	320	215	74	170	320	228	65	180	240	198	27	160	300	250	78	
Zr	90	100	95	6	80	220	138	66	110	280	168	78	140	180	160	28	
Sr	20	30	23	6	30	30	30	0	30	30	30		20	20	20		
Rb	20	30	25	7	20	20	20	0	20	20	20	0	20	20	20		
As	80	180	110	47	80	140	115	30	90	200	124	44	50	140	100	46	
Ni	BDL	BDL	BDL	BDL	BDL	BDL	BDL	BDL	540	540	540		BDL	BDL	BDL	BDL	
Mn	590	590	590		790	790	790		770	770	770		BDL	BDL	BDL	BDL	
Pb	50	90	68	17	60	60	60	0	50	70	64	9	40	60	53	12	
	Heterolithic core (n=3)				Elongated (n=4)				HF (n=2)				oxidised (n=4)				Coarse grain
Fe ₂ O ₃	11.3	31.7	21.4	10.2	14.7	31.3	25.6	7.4	4.4	7.9	6.1	2.4	11.4	28.7	23.4	8.0	18.2
TiO ₂	0.48	0.48	0.48		BDL	BDL	BDL	BDL	0	0			0.33	0.33	0.33		BDL
CaO	0.09	0.10	0.09	0.01	0.08	0.10	0.09	0.01	0.08	0.09	0.08	0.01	0.08	0.14	0.11	0.03	0.12
K ₂ O	0.02	0.09	0.04	0.04	0.02	0.46	0.13	0.22	0.02	0.02	0.02	0.00	0.02	0.3	0.09	0.14	0.02
SiO ₂	2.9	9.43	6.17	3.27	7.7	9.4	8.4	0.8	10.6	11.7	11.1	0.8	5.7	12.0	7.7	3.0	14.6
∑ S	7.1	16.7	12.3	4.8	1.0	14.3	9.4	6.1	7.7	15.1	11.9	3.2	8.4	9.6	9.0	0.8	13.969
Cl	0.1	0.1	0.1	0.0	0.1	0.1	0.1	0.0	0.1	0.1	0.1	0.0	0.1	0.1	0.1	0.0	0.1
Total	22	58	40	18	25	54	44	13	24.8	28.3	26.5	2.5	32	52	43	8	47
Mo	200	420	323	112	200	330	243	59	110	140	125	21	260	510	368	104	140
Nb	220	1260	630	554	240	310	275	49	210	230	220	14	210	890	470	293	140
Zr	520	990	755	332	70	90	80	14	60	110	85	35	120	280	180	73	BDL
Sr	20	40	30	10	40	40	40		BDL	BDL	BDL	BDL	30	60	40	17	20
Rb	20	20	20		20	40	30	14	BDL	BDL	BDL	BDL	20	30	27	6	BDL
As	220	570	395	247	80	150	110	36	BDL	BDL	BDL	BDL	80	200	137	60	70
Ni	BDL	BDL	BDL	BDL	BDL	BDL	BDL	BDL	BDL	BDL	BDL	BDL	420	1020	720	424	
Pb	70	70	70	0	50	70	58	10	40	40	40	0	50	80	63	15	60

Thus, the spherical or nearly spherical concretions from the Tukau Formation indicate that they had evenly grown in isotropic media. The spherical shape concretions are formed nearly isotropic qualities since the movement of solution within the sandstone is normal while the solution mobility is restricted in the vertical direction leading to anisotropic qualities, results flattened shapes (Butts and Moore, ND). The different size populations of concretions may represent discrete reaction fronts with varying reactant supplies (Potter et al., 2011). Elongate and tabular concretions are parallel to sedimentary strata and have been reported, that these structures are due to the influence of saturated (phreatic zone) groundwater flow direction which might have been on the orientation of the axis of elongation (Mozley and Davis, 2005). No doublets and triplet concretions were observed from the studied sections. Mostly the concretions are solid and micro and macro laminations were observed.

Table 3. Comparison of the chemistry of concretions with the bulk geochemistry of the sediments of the Tukau Formation (Nagarajan et al., 2017a).

Elements	Concretion (n=30)	*Whole rock (n=63 & 50 for major and trace elements respectively)
SiO ₂	9.15	78.51
TiO ₂	0.41	0.64
Al ₂ O ₃	BDL	12.08
Fe ₂ O _{3t}	24.49	1.99
MnO	0.09	0.01
MgO	BDL	0.48
CaO	0.09	0.07
Na ₂ O	BDL	0.06
K ₂ O	0.05	1.81
P ₂ O ₅	BDL	0.03
Total S	12.60	ND
Cl	0.13	ND
Rb ppm	23.6	81.38
Sr ppm	30.0	50.60
Ba ppm	BDL	177.86
Y ppm	BDL	19.52
Zr ppm	186.7	231.68
V ppm	BDL	70.22
Cr ppm	BDL	74.19
Co ppm	BDL	6.94
Ni ppm	660.0	32.14
Cu ppm	BDL	41.32
Zn ppm	BDL	60.56
Th ppm	ND	9.87
Pb ppm	60.7	16.34
Mo ppm	293.3	ND
As ppm	136.8	8.03
Nb ppm	300.4	6.00

Comparison with Source rock chemistry

The geochemical characteristics of the Tukau Formation are not well addressed for the whole formation yet; however, a recent study by Nagarajan et al. (2017a) addressed the geochemical characteristics of the clastic sediments from the upper part of the formation, which was compared with the geochemistry of the concretions (Table 3). Source rocks mainly consist of sandstone, shale interbedded with coal and some conglomerate beds. Source rocks are enriched with SiO₂, TiO₂, Al₂O₃, K₂O, MgO Na₂O, P₂O₅, Rb, Sr, V, Ba, Cr, Co, Cu and Zn compared to concretions and CaO is comparable between them. These host sediments are moderate to intensively weathered in the source region, and recycled nature with minor input of mafic rocks (Nagarajan et al., 2014; 2017a). Concretions are enriched with Fe₂O₃, MnO, SO₄, Zr, Ni, Pb, Mo, As and Nb compared to that of the source rocks. The enrichment factor (EF) was calculated to understand the relationship between concretions and the host sediments by dividing the concentration in concretions by the same in the host sediments.

Table 4. Pearson's correlation coefficient for the geochemistry of pyrite concretions from the Tukau Formation.

Elements	Fe ₂ O ₃	CaO	K ₂ O	SiO ₂	S	Cl	Mo	Nb	Zr	Sr	Rb	As	Pb
Fe ₂ O ₃	1												
CaO	-0.39	1											
K ₂ O	-0.91	0.55	1										
SiO ₂	-0.41	0.15	0.47	1									
S	0.89	-0.42	-0.84	-0.28	1								
Cl	0.56	0.41	-0.45	-0.17	0.51	1							
Mo	0.52	0.43	-0.27	-0.23	0.19	0.64	1						
Nb	-0.42	0.6	0.46	-0.47	-0.57	-0.03	0.27	1					
Zr	-0.3	-0.08	0.18	-0.39	0.03	-0.28	-0.6	0.3	1				
Sr	0.11	0.11	0.19	-0.03	-0.15	-0.19	0.47	0.18	-0.39	1			
Rb	0.36	-0.18	-0.25	-0.41	-0.03	0.01	0.58	0.3	-0.36	0.45	1		
As	0.45	-0.2	-0.37	-0.67	0.61	0.14	0.04	0.14	0.65	-0.01	0.1	1	
Pb	0.45	0.1	-0.24	-0.26	0.46	0.33	0.49	0.14	0.15	0.08	0.4	0.66	1

Based on the calculated values of EF, concretions are enriched with Fe₂O₃ (12 fold; n=30); Ni (20 fold: n=3); Mn (10 fold: n=3); Pb (4 fold; n=30). Even though Ni and Mn show significant enrichment in concretions, these elements were recorded only in three concretion samples. Same time, EF values were not calculated for total S, since the concentration of total sulphur in the host rock was not available. Other elements such as Sr, Rb, Zr, Ca, and SiO₂ show very low values of enrichment, normally less than 2. Mineralogically all the concretions except four samples consisting of quartz and pyrite. The four samples show different mineralogy (Quartz with other minerals such as pyrite (FeS₂) Catterite (CoS₂), Goethite (FeOOH), Berlinite (AlPO₄) and Pyrite arsenian ((Fe,As)S₂). Catterite and arsenian pyrite are the varieties of pyrite, where, they contain Co and As respectively. Arsenic has both chalcophile and siderophile characteristics, and tends to be hosted by sulphide minerals such as pyrite or hydroxidic Fe phases like goethite, both can host As up to several wt.% (Smedley and Kinniburgh, 2002). Cationic substitution is common in pyrite, with several metals readily substituting Fe. Often, Co, Ni, Mn, Ag, and Au can substitute in sufficient quantity; which can influence in density, hardness, and color of concretions. Particularly, Co readily substitutes Fe and vice-versa that pyrite forms a solid-solution series with catterite (cobalt disulfide, CoS₂), and the intermediate varieties are called cobaltian pyrite. Raiswell and Plant (1980) investigated the incorporation of trace elements into pyrite during diagenesis of black shales from Yorkshire and found that trace elements concentration was extremely low except for some sulphur phase trace elements (Cu, As, Mo, Ni, Zn, and Co). Arsenic in the environment is mainly controlled by the predominant physico-chemical conditions and the presence of other ions. Also, as behaviour (adsorption, desorption, transport, and redox transformation) is governed by crucial parameters such as redox potential, pH and ionic competition. Reducing environmental conditions mainly leads to mobilization from oxides whereas oxidizing conditions may mobilize to sulphides (Smedley and Kinniburgh, 2002). Molybdenum, arsenic and selenium commonly occur in pyrite (sulphides; Fleischer, 1955). Molybdenum is a common constituent of petroleum and it seems to be present in organometallic compounds (Rankama and Sahama, 1950). A reduction environment can boost the enrichment of Mo in a shallow environment where there is contact near the oxic-anoxic interface (Adelson et al., 2001).

Statistical analysis

Iron shows a strong positive correlation with total sulphur (r=0.89) indicating these elements are associated together with mineral pyrite in concretion (Table 4). Mo and Cl also show a moderated positive correlation with Fe₂O₃, which further confirms that these elements are associated with pyrite in concretion and also the pyrite is precipitated in sub-anoxic interface. K₂O shows a strong negative relationship with Fe₂O₃ and total sulphur (r= -0.91 and -0.84; Table 4), indicating that K₂O is associated with clay materials and not with pyrite. SiO₂, CaO, Rb, and Sr do not show any strong relationship with

either Fe₂O₃ or total sulphur (Table 4), indicating that these elements are not linked with pyrite precipitation in concretion and are related to quartz, microfossils, clay materials and/or with organic matter, which forms nucleus in many concretions. Trace elements can present in pyrite in the form of nano-particles, adsorbed films and as micro and nano inclusions during coprecipitation with pyrite (Wohlgenuth-Ueberwasser et al., 2015; (Bethke and Barton, 1971; Grant et al., 2018) and many trace elements are enriched in pyrite/coal together with total S (e.g. Song et al., 2007; Sia and Abdullah, 2011). Pb shows a weak correlation with total sulphur and Mo which indicates that Pb occurrence in the concretion is associated with Pyrite. Sr is mostly associated with calcite but calcite is so sparse in these concretions, thus might be controlled by other phases (weak positive correlation with Rb). The original relationship of Co, Ni, Zn with S may be modified during the oxidation of pyrite. As and Pb show low to moderate positive correlation with total sulphur (r=0.61 and 0.46 respectively) and moderate correlation between them (r=0.66) indicating their association with sulphur.

The varimax rotation method was used to maximize the sum of the variance (Gotelli and Ellison 2004) and is shown in Figure 4. Factor 1 is accounted for 29.09% of the total variance and is characterized by high positive loadings of K₂O and Nb and high negative loadings of Fe₂O₃ and S. Factor 2 is accounted for 22.02% of the total variance and is characterized by high negative loading of SiO₂ and positive loadings of As, and Zr (Fig. 4). Moderate positive loading of Pb in Factor 2 may be similar to the process of As and would have controlled by the zircon grains but less extent compared to As. SiO₂ is related to quartz grains in concretion, which do not incorporate any sulphide group of elements such as As and Pb. Factor 3 is defined by four elements and accounts for 18.36% of the total variance. In which Sr, Rb and Mo are loaded positively (strong to moderate) whereas Zr is loaded negatively. Zr may be associated with detrital minerals such as zircon. As stated above, CaO, Rb, and Sr do not show any relationship with either Fe₂O₃ or total sulphur, indicating that these elements were not linked with pyrite concretions in concretion and are related to parent materials or can be associated with organic matter which forms nucleus or inter laminated in many concretions. Factor 4 accounted for 18.20% of the total variance and is characterized by Cl, MO and CaO. The close association of Cl and Mo in the studied concretions may indicate the redox front environment, in which Mo and Cl are incorporated with pyrite during the precipitation of pyrite concretion. Mo and Cl moderated positive correlation with Fe₂O₃, which further confirms that these elements are associated with pyrite in concretion and also the pyrites were precipitated in a sub-anoxic interface. CaO is loaded in factors 1 and 4 and may be associated with the presence of microfossils in the nucleus, however, which are not observed in the petrographic study as the nucleus did not sustain during the preparation of the thin sections.

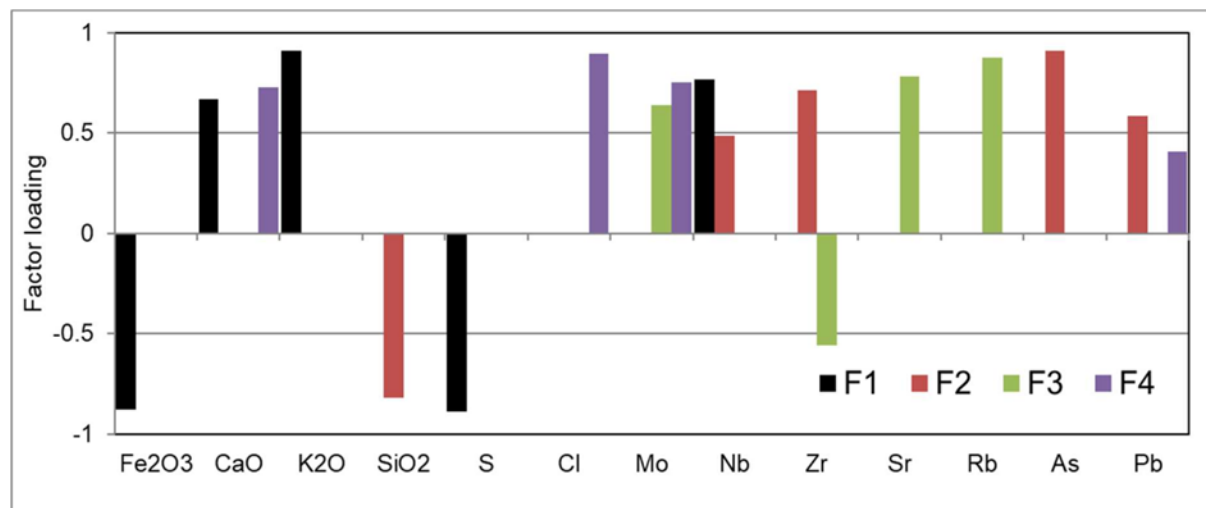


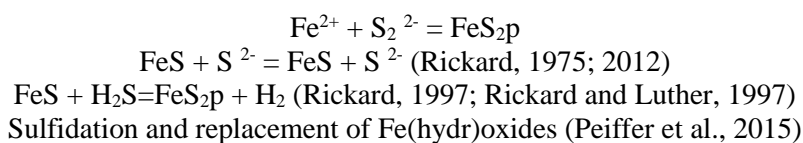
Fig. 4. Varimax rotated component matrix factor model for the concretions of the Tukai Formation.

Mechanism of formation

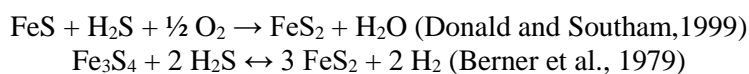
Concretions form in common sedimentary rocks such as shale, siltstone, mudstone, and sandstone when minerals that have dissolved in groundwater precipitate around a nucleus. Concretion formation

requires that reactants should reach some extent of super-saturation (e.g. nucleation threshold) with respect to equilibrium precipitation (Chan et al., 2007). The principal controlling factors on pyrite formation within the sediments are the type and amount of organic matter, reactive iron minerals and the availability of dissolved sulphate. Pyrite concretions occur as a minor constituent of many rocks and are normally abundant in organic matter-rich rocks such as black shale, oil shale, and coals (Berner 1970). Such mineral formation is the result of saturated ion concentrations (Wilkin and Arthur, 2001) and/or early diagenetic processes such as the decomposition of organic matter and microbial activity (Berner, 1981; Beveridge et al., 1983). In general, pyrite occurrences are indicative of anoxic conditions, sulphate reduction, and high organic carbon burial flux (Heggie, 1992). Pyrite concretions begin their development when iron- and sulphur -rich groundwater precipitate pyrite around carbon particles to form tiny “seed” crystals. These seed crystals promote further pyrite precipitation which, in proper conditions of chemistry and temperature, slowly accumulates into concretions.

Pyrite (FeS₂) is considered as a common product of early diagenesis in organic-rich sediments which can be achieved by the reaction of sulfide (through bacterial sulphate reduction,) with either Fe(III) in sediments or Fe(II) produced by bacterial Fe(III) reduction (Berner, 1970; Lovley, 1991). The fundamental reactions for the pyrite nucleation and growth is just opposite to the congruent dissolution reaction. That is:



Also, it is stated that iron sulfide formation in sedimentary environments is related to Iron monosulphide and poly-sulphide reactions. First, iron monosulphide (FeS) precipitates in the subsurface of the sediments under reducing conditions by a reaction between dissolved ferrous Fe and sulphide. This Fe-monosulphide is pervasive in surficial marine sediments however, it is rapidly replaced by the stable diagenetic end-member pyrite (FeS₂), which is achieved through the dissolution of FeS and subsequent reactions with dissolved H₂S or intermediate oxidation state of sulphur species such as polysulphides (Rickard, 1975; Rickard and Luther, 1997). As a result, pyrite establishes a primary long-term marine sink for Fe and S (Berner, 1970). Sulphate-reducing bacteria also can be involved in the formation of pyrite under sub- to anoxic, organic-rich environments. The H₂S produced by sulphate-reducing bacteria and the interaction between Fe²⁺ and anionic groups on the cell surface can enhance the precipitation of FeS (Southam et al., 2001). Bacterial sulphate production provides sulphide ions (HS⁻ and H₂S), which react with dissolved iron to form pyrite either directly or via an iron monosulphide precursor (Berner, 1984; Schoonen, 2004). Sulphate reduction may lead to the formation of acidity, which is confirmed by the low pH recorded for the host sediments. The necessary Fe may be derived from terrigenous clastic sediments, where iron is coated as oxyhydroxide on terrigenous particles (Berner, 1969; Schieber, 2007) and or exchangeable cations in clays. Pyrite cannot form directly without higher levels of supersaturation, trace element reactivity, or the presence of active surfaces. However, more pyrite will precipitate more rapidly and with a lower concentration of reactants if there are pyrite seed crystals available (Harmandas et al., 1998). Similarly, the amount of pyrite supersaturation required can be reduced by the incorporation of trace elements; for example, it has been demonstrated that the presence of Ni significantly reduces the time required for pyrite growth (Morin et al., 2017). To form pyrite at low temperatures iron monosulphides should overcome a kinetic barrier (Berner 1970, Southam and Saunders, 2005). This can be possible through a series of soluble intermediates or by partial oxidation of hydrogen sulphide under sub-anoxic conditions, which can be shown as follows for sub-oxic to anoxic conditions.



Additionally, the precipitation of the hydrous ferric oxide (goethite in concretions) requires a chemical environment with oxidizing conditions. The replacement of Fe(hydr)oxides (e.g., lepidocrocite, ferrihydrite and goethite) and sulfidation is another possibility for the formation of pyrite (Peiffer et al.,

2015). In this mechanism, the Fe^{3+} is converted into Fe^{2+} together with the reaction with polysulphide to form pyrite and possibly with the help of FeS precursor (Peiffer et al., 2015). The above mechanism would aid the formation of nodules in two different ways. The species of polysulphide is known to adsorb onto the surfaces of the Fe (hydr)oxide pre-existing species. This would result in the precipitation of FeS that would take place close to the location of Fe(hydr)oxide species even being replaced by solid phase transformation (Peiffer et al., 2015). The second would be the reduction of Fe(hydr)oxide due to diagenetic processes that would result in the production of $\text{Fe}^{2+}(\text{aq})$. This aqueous might lead to the areas of pyrite seed crystals or induce a higher concentration of polysulphides/ H_2S to react to form the pyrite nodules. Some concretions show the presence of goethite might have gone for oxidation.

Conclusion

A preliminary attempt was made on the concretions from the Tukai Formation, NW Borneo, Sarawak, Malaysia. Basic mineralogical and geochemical characteristics have been documented for the first time in the Tukai Formation. The concretions from the Tukai formation are classified as circular, elongated, tabular, spherical, heterolithic, and irregular based on their shapes and geometry. Nucleus and layers are observed in spherical and irregularly shaped concretions respectively, which look like organic matter. Mineralogically these concretions consist of pyrite and quartz minerals with the rare occurrence of catterite, goethite, berlinite, and arsenopyrite. Chemically these concretions are enriched with Fe_2O_3 , SiO_2 , total sulphur, and trace metals such as Mo, As, and Pb. Ni and Mn are recorded higher in selected samples. Trace elements are mostly associated with sulphur and Fe_2O_3 and are controlled by pyrite. Based on this study, it is observed that these concretions would have formed under significantly reducing conditions (microbial sulphate reduction) during early diagenesis or replacement of Fe(hydr)oxides and the sulfidation mechanism with the aid FeS precursor during the diagenetic processes. However, a further detailed study should be carried out to confirm the diagenetic paleoenvironments of these pyrite concretions from the Tukai Formation.

Acknowledgments

The first author would like to thank our final year Applied Geology students for their help in the collection of concretions from the Tukai Formation during their field trip and final year project work. The authors are grateful to the reviewers for their reviews and suggestions on the manuscript and the Editor for the invitation to contribute.

References

- Adelson, J.M., Helz, G.R. and Miller, C.V. (2001) Reconstructing the rise of recent coastal anoxia molybdenum in Chesapeake Bay sediments. *Geochimica et Cosmochimica Acta*, v.65, pp.237–252.
- El Albani, A., Vachard, D., Kuhnt, W. and Thurow, J. (2001) The role of diagenetic carbonate concretions in the preservation of the original sedimentary record. *Sedimentology*, v.48(4), pp.875–886.
- Baird, G.C., Sroka, S.D., Shabica, C.W. and Kuecher, G.J. (1986) Taphonomy of middle Pennsylvanian Mazon Creek Area fossil localities northeast Illinois, USA: significance of exceptional fossil preservation in syngenetic concretions. *Palaios*, v.1(3), pp.271–285.
- Berner, R.A., Baldwin, T. and Holdren, G.R. (1979) Authigenic iron sulfides as paleosalinity indicators. *Journal of Sedimentary Petrology*, v.49(4), pp.1345–1350.
- Berner, R.A. (1969) Synthesis of framboidal pyrite. *Economic Geology*, v.64, pp.383–384.
- Berner, R.A. (1970) Sedimentary pyrite formation. *American Journal of Science*, v.268, pp.1–23.
- Berner, R.A. and Raiswell, R. (1983) Burial of organic carbon and pyrite sulfur in sediments over Phanerozoic time: a new theory. *Geochimica et Cosmochimica Acta*, v.47, pp.855–862.
- Berner, R.A. (1981) Authigenic mineral formation resulting from organic matter decomposition in modern sediments. *Fortschritte der Mineralogie*, v.59, pp.117–135.
- Berner, R.A. (1984) Sedimentary pyrite formation: an update. *Geochimica et Cosmochimica Acta*, v.48, pp.605–615.
- Bethke, P.M. and Barton, P.B. (1971) Distribution of some minor elements between coexisting sulfide minerals. *Economic Geology*, v.66, pp.140–163.
- Beveridge, T.J., Meloche, J.D., Fyfe, W.S. and Murray, R.G.E. (1983) Diagenesis of metals chemically complexed to bacteria: laboratory formation of metal phosphates, sulfides, and organic condensates in artificial sediments. *Applied and Environmental Microbiology*, v.45, pp.1094–1108

- Bowen, B., Benison, K.C., Oboh-Ikuenobe, F.E., Story, S. and Mormile, M.R. (2008) Active hematite concretion formation in modern acid saline lake sediments, Lake Brown, Western Australia. *Earth and Planet. Sci. Lett.*, v.268, pp.52–63.
- Butts, C. and Moore, E.S. (ND) *Geology and Mineral Resources of the Bellefonte Quadrangle, Pennsylvania*. USGS Bulletin. 855 (out of Print).
- Chan, M., Parry, W.T. and Bowman, J.R. (2000) Diagenetic hematite and manganese oxides and fault- related fluid flow in Jurassic sandstones, southeastern Utah. *AAPG Bull.*, v.84, pp.1281–1310.
- Chan, M., Parry, W., Beitler, B., Ormö, J. and Komatsu, G. (2004) A possible terrestrial analogue for haematite concretions on Mars. *Nature*, v.429, pp.731–734.
- Chan, M., Bowen, B., Parry, W., Ormö, J. and Komatsu, G. (2005) Red rock and red planet diagenesis; comparisons of Earth and Mars concretions. *GSA Today*, v.15, pp.4–10.
- Chan, M.A., Ormoe, J., Park, A.J., Stich, M., Souza-Egipsy, V. and Komatsu, G. (2007) Models of iron oxide concretion formation; field, numerical, and laboratory comparison. *Geofluids*, v.7, pp.356–368.
- Coleman, M. (2005) Processes of Formation of spheroidal concretions and inferences for “Blueberries” in Meridiani Planum sediments. In 36th Lunar and planetary science (IPSC) abstracts, #2148.
- Coleman, M.L. and Raiswell, R. (1981) Carbon, oxygen and sulphur isotope variations in concretions from the upper Lias of N.E. England. *Geochimica et Cosmochimica Acta*, v.45, pp.329–340.
- Coleman, M. and Raiswell, R. (1995) Source of carbonate and origin of zonation in pyritiferous carbonate concretions; evaluation of a dynamic model. *American Jour. Sci.*, v.295, pp.282–308.
- Donald, R. and Southam, G. (1999) Low temperature anaerobic bacterial diagenesis of ferrous monosulfide to pyrite. *Geochimica et Cosmochimica Acta*, v.63, pp.2019–2023.
- Driscoll, E.G., Hall, D.D. and Nussmann, D.G. (1965) Morphology and paleoecology of the brachiopod *Leiorhynchus kelloggi* Hall, Middle Devonian, Ohio, Michigan, Ontario. *Jour. Paleontology*, v.39, pp.916-933.
- Ehinola, O.A., Shengfei, Q. and Onibonoje, A.A. (2010) The Paleoenvironmental Significance of Pyritic Nodules from Lokpanta Oil Shale Interval In The Petroleum System of Lower Benue Trough, Nigeria. *Petroleum & Coal*, v.52, pp.110-122,
- England, G.L., Rasmussen, B., Krapez, B. and Groves, D.I. (2002) Palaeoenvironmental significance of rounded pyrite in siliciclastic sequences of the late Archean Witwatersand Basin: Oxygen deficient atmosphere or hydrothermal alteration? *Sedimentology*, v.49, pp.1133-1159.
- Fleischer, M. (1955) Minor elements in some sulfide minerals: *Econ. Geol.*, 53th Anniv.1905-1955, pp.970-1024.
- Gotelli, N. J. and Ellison, A. M. (2004) *A Primer of Ecological Statistics*. I (Ed), Sunderland, MA, USA: Sinauer Associates, 492p.
- Grant, H.L.J., Hannington, M.D., Petersen, S., Frische, M. and Fuchs, S.H. (2018) Constraints on the behavior of trace elements in the actively-forming TAG deposit, Mid-Atlantic Ridge, based on LA-ICP-MS analyses of pyrite. *Chem. Geology*, v.498, pp.45-71
- Harmandas, N.G., Navarro Fernandez E. and Koutsoukos, P.G., (1998) Crystal growth of pyrite in aqueous solutions. Inhibition by organophosphorus compounds. *Langmuir*, v.14, pp.1250 – 1255.
- He, Q., An, Y., Sun, F. and Lai, C., 2019. Genesis of pyrite concretions: Constraints from mineral and geochemical features of Longtan Formation in Anhui Province, eastern China. *Minerals*, v.9, p.467.
- Heggie, D.T. (1992) Organic matter and paleochemistry of cretaceous sediments from the argo and gascoyne abyssal plains, northeastern indian ocean. *Proceedings of the Ocean Drilling Prog. Scientific Results*, v.123, pp.225-236.
- Huggett, J.M. (1994) Diagenesis of mudrocks and concretions from the London Clay Formation in the London Basin. *Clay Mineralogy*, v.29, pp.693–707.
- Hutchison, C.S. (2005) *Geology of North-West Borneo; Sarawak*. In: Brunei and Sabah. Elsevier, Amsterdam.
- Jayaprakash, M., Ramasamy, N., Velmurugan, P., Giridharan, L., Neetha, V. and Urban, B. (2014) Geochemical Assessment of Sediment Quality using Multivariate Statistical Analysis of Ennore Creek, North of Chennai, SE Coast of India. *Pertanika Jour. Sci. Tech.*, v.22, pp.303 –316.
- Kaiser, H. F. (1960) The application of electronic computers to factor analysis. *Educational and Psychological Measurement*, v.20, pp.141-151.
- Kessler, F.L. and Nagarajan, R. (2012) A semi-quantitative assessment of clay content in sedimentary rocks using portable X-ray fluorescence spectrometry. *Int. Jour. Earth Sci. Eng.*, v.05, pp.363–364.
- Kessler F.L. and Nagarajan, R. (2013) Rubidium detected with X-ray fluorescence spectrometry: a new semi-quantitative assessment of clay content in sedimentary rocks. *Warta Geologi*, v.39, pp.27- 30.
- Kessler, F.L. (2010) Observations on sediments and deformation characteristics of the Sarawak Foreland, Borneo Island. *Warta Geologi*, v.35, pp.1–10.
- Liechti, P.R., Roe, F.W. and Haile, N.S. (1960) The geology of Sarawak, Brunei and the western part of North Borneo. *British Borneo Geol. Surv. Bull.*, v.3, pp.1–360.
- Lovley, D.R. (1991) Dissimilatory Fe (III) and Mn (IV) reduction. *Microbiology Rev.*, v.55, pp.259- 287.

- Lozano, R. and Bernal, J.P. (2005) Characterization of a new set of eight geochemical reference materials for XRF major and trace element analysis. *Revista Mexicana de Ciencias Geológicas*, v.22, pp.329–344.
- Milliken, K.L., McBride, E.F., Cavazza, W., Cibin, U., Fontana, D., Picard, M.D. and Zuffa, G.G. (1998) Geochemical history of calcite precipitation in Tertiary sandstones, Northern Apennines, Italy. In: Morad, S. (Ed.), *Carbonate Cementation in Sandstones*. v.26, pp.213–240.
- Mozley, P. and Davis, J.M. (2005) Internal structure and mode of growth of elongate calcite concretions; evidence for small-scale, microbially induced, chemical heterogeneity in groundwater. *Geol. Soc. America Bulletin*, v.117, pp.1400–1412.
- Mozley, P.S. (1989) Relation between depositional environment and the elemental composition of early diagenetic siderite. *Geology*, v.17, pp.704-706.
- Nagarajan, R., Roy, P.D., Jonathan, M.P., Lozano, R., Kessler, F.L. and Prasanna, M.V. (2014) Geochemistry of Neogene sedimentary rocks from Borneo Basin, East Malaysia: Paleo- weathering, provenance and tectonic setting. *Chemie der Erde-Geochemistry*, v.74, pp.139-146.
- Nagarajan, R., Armstrong-Altrin, J.S., Kessler, F.L., Hidalgo-Moral, E.L., Dodge-Wan, D. and Taib, N.I. (2015) Provenance and tectonic setting of Miocene siliciclastic sediments, Sibuti Formation, northwestern Borneo. *Arabian Jour. Geosci.*, v.8, pp.8549-8565.
- Nagarajan, R., Roy, P.D., Kessler, F.L., Jong, J., Dayong, V. and Jonathan, M.P. (2017a) An integrated study of geochemistry and mineralogy of the Upper Tukau Formation, Borneo Island (East Malaysia): Sediment Provenance, Depositional Setting and Tectonic Implications. *Jour. Asian Earth Sci.*, v.143, pp.77-97.
- Nagarajan, R., Behrends, T., Hellige, K., Larese-Casanova, P., Wan, M. and Pollok, K. (2017b) Provenance of the Neogene sedimentary rocks from the Tukau and Belait Formations, Northeastern Borneo by mineralogy and geochemistry. *Warta Geologi.*, v.43, pp.10-16.
- Pantin, H.M. (1958) Rate of formation of a diagenetic calcareous concretion. *Jour. Sedimentary Petrology*, v.28, pp.366–371.
- Peiffer, S., et a Behrends, T., Hellige, K., Larese-Casanova, P., Wan, M. and Pollok, K. (2015) Pyrite formation and mineral transformation pathways upon sulfidation of ferric hydroxides depend on mineral type and sulfide concentration. *Chemical Geology*, v.400, pp.44-55.
- Potter, S L., Chan, M.A., Petersen, E.U., Dyar, M.D. and Sklute, E. (2011) Characterization of Navajo Sandstone concretions: Mars comparison and criteria for distinguishing diagenetic origins. *Earth and Planetary Sci. Lett.*, v.301, pp.444–456.
- Pye, K., Dickson, J.A.D., Schiavon, N., Coleman, M.L. and Cox, M. (1990) Formation of siderite- Mg-calcite-iron sulphide concretions in intertidal marsh and sandflat sediments, north Norfolk, England. *Sedimentology*, v.37, pp.325-343.
- Raiswell, R. and Plant, J. (1980) The incorporation of trace elements into pyrite during diagenesis of Black shales, Yorkire, England. *Economic Geology*, v.75, pp.684-699.
- Raiswell, R. (1976) The microbiological formation of carbonate concretions in the upper Lias of NE England. *Chemical Geology*, v.18, pp.227–244.
- Raiswell, R. and Fisher, Q.J. (2004) Rates of carbonate cementation associated with sulphate reduction in DSDP/ODP sediments: implications for the formation of concretions. *Chemical Geology*, v.211, pp.71-85.
- Raiswell, R. and Fisher, Q.J. (2000) Mudrock-hosted carbonate concretions; a review of growth mechanisms and their influence on chemical and isotopic composition. *Jour. Geol. Soc. London*, v.157, pp.239–251.
- Ramkumar, M., 2001. Sedimentary environments of the modern Godavari delta: characterization and statistical discrimination towards computer assisted environment recognition scheme. *Jour. Geol. Soc. India*, v.57, pp.49–63.
- Rankama, K. and Sahama, Th. G. (1950) *Geochemistry*. Chicago, Chicago Univ. Press. 912 p.
- Rickard, D. (1997) Kinetics of pyrite formation by the H₂S oxidation of iron (II) monosulfide in aqueous solutions between 25 and 125 °C: The rate equation. *Geochimica et Cosmochimica Acta*, v.61, pp.115-134.
- Rickard, D. (2012) *Sulfidic Sediments and Sedimentary Rocks*, Elsevier.
- Rickard, D. and Luther, G. W. (1997). Kinetics of pyrite formation by the H₂S oxidation of iron (II) monosulfide in aqueous solutions between 25 and 125°C, The mechanism. *Geochimica et Cosmochimica Acta*, v.61, pp.135-147.
- Rickard, D.T. (1975) Kinetics and mechanism of pyrite formation at low-temperatures. *American Jour. Sci.*, v.275, pp.636–652.
- Roy, P.D., Morton-Bermea, O., Hernández-Álvarez, E., Pi, T. and Lozano, R. (2010) Rare earth element geochemistry of the Late Quaternary tephra and volcano-clastic sediments from the Pachuca sub- basin, north-eastern Basin of Mexico. *Geofísica Int.*, v.49, pp.3–15.
- Schieber, J. (2007) Oxidation of detrital pyrite as a cause for Marcasite Formation in marine lag deposits from the Devonian of the eastern US. *Deep-Sea Research II*, v.54, pp.1312–1326.

- Schoonen, M.A.A. (2004) Mechanisms of sedimentary pyrite formation. In: Lyons, T.W. (Ed.), *Sulfur Biogeochemistry- Past and Present*. Geol. Soc. America Special Paper, pp.117–134.
- Seilacher, A. (2001) Concretion morphologies reflecting diagenetic and epigenetic pathways. *Sedimentary Geol.*, v.143, pp.41–57.
- Sia, S. and Abdullah, W.H. (2011) Concentration and association of minor and trace elements in Mukah coal from Sarawak, Malaysia, with emphasis on the potentially hazardous trace elements. *Int. Jour. Coal Geol.*, v.88, pp.179-193.
- Smedley P.L. and Kinniburgh, D.G. (2002) A review of the source, behavior and distribution of arsenic in natural waters. *Applied Geochemistry*, v.17, pp.517-568.
- Song, D., Qin, Y., Zhang, J., Wang, W. and Zheng, C. (2007) Concentration and distribution of trace element in some coals from Northern China. *Int. Jour. Coal Geol.*, v.69, pp.179-191.
- Southam, G. and Saunders, J.A. (2005) The geomicrobiology of ore deposits. *Economic Geology*, v.100, pp.1067-1084.
- Southam, G., Brock, C., Donald, R. and Røstad, A. (2001) Pyrite discs in coal: evidence for fossilized bacterial colonies. *Geology*, v.29, pp.47-50.
- Verma, S.P., Lozano-SantaCruz, R., Girón, P. and Velasco, F. (1996) Calibración preliminar de Fluorescencia de Rayos X para análisis cuantitativo de elementos trazas en rocas ígneas. *Actas INAGEQ 2*, pp.231–242.
- Wilford, G.E. (1961) The geology and mineral resources of Brunei and adjacent parts of Sarawak. With Descriptions of the Seria and Miri Oilfields. *British Geol. Sur. Mem. 10*. Brunei Press Limited, Brunei.
- Wilkin, R.T. and Arthur, M.A. (2001) Variations in pyrite texture, sulfur isotope composition, and iron systematics in the Black Sea: evidence for Late Pleistocene to Holocene excursions of the O₂- H₂S redox transition. *Geochimica et Cosmochimica Acta*, v.65, pp.1399–1416.
- Wilson, J.H., McLennan, S.M., Glotch, T.D., Rasbury, E.T., Gierlowski-Kordesch, E.H. and Tappero, R.V. (2012) Pedogenic hematitic concretions from the Triassic New Haven Arkose, Connecticut: Implications for understanding Martian diagenetic processes. *Chemical Geology*, v.312, pp.195-208.
- Wohlgemuth-Ueberwasser, C.C., Viljoen, F., Petersen, S. and Vorster, C. (2015) Distribution and solubility limits of trace elements hydrothermal black smoker sulfides: An in-situ LA-ICP-MS study. *Geochimica et Cosmochimica Acta*, v.159, pp.16-41.
- Woodland, B.G. and Stenstrom, R.C. (1979) The occurrence and origin of siderite concretions in the Francis Creek Shale (Pennsylvanian) of northeastern Illinois, in Nitecki, M.H., ed., *Mazon Creek fossils*: New York, NY, Academic Press, pp.69-103.
- Xu., H., Hou, D., Lohr, S.C., Liu, Q. and George, S.C. (2020) Early diagenetic pyrite cementation influences molecular composition of sedimentary organic matter in the Dongying Depression, China. *Organic Geochemistry*, v.144, p.104019.

Manuscript received: 02-10-2022

Manuscript accepted: 05-12-2022